Communication

Chiral Periodic Mesoporous Organosilicates Based on Axially Chiral Monomers: Transmission of Chirality in the Solid State

Stephanie MacQuarrie, Matthew P. Thompson, Alexandre Blanc, Nicholas J. Mosey, Robert P. Lemieux, and Cathleen M. Crudden

J. Am. Chem. Soc., **2008**, 130 (43), 14099-14101 • DOI: 10.1021/ja804866e • Publication Date (Web): 03 October 2008

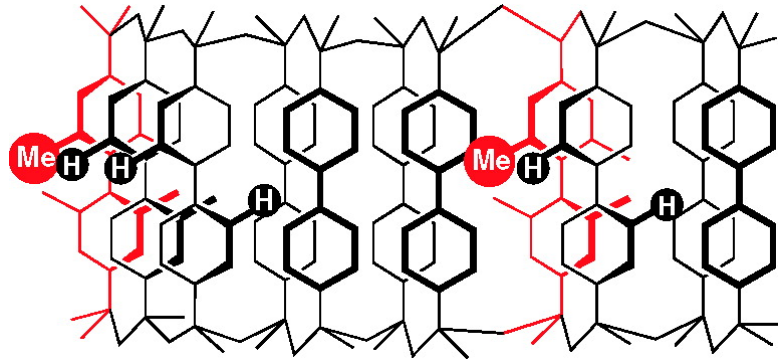

More About This Article

Additional resources and features associated with this article are available within the HTML version:

- Supporting Information
- Access to high resolution figures
- Links to articles and content related to this article
- Copyright permission to reproduce figures and/or text from this article

View the Full Text HTML

J|A|C|S
COMMUNICATIONS

Published on Web 10/03/2008

Chiral Periodic Mesoporous Organosilicates Based on Axially Chiral Monomers: Transmission of Chirality in the Solid State

Stephanie MacQuarrie, Matthew P. Thompson, Alexandre Blanc, Nicholas J. Mosey, Robert P. Lemieux, and Cathleen M. Crudden*

Department of Chemistry, Queen's University, 90 Bader Lane, Kingston, Ontario, Canada K7L 3N6

Received June 25, 2008; E-mail: cruddenc@chem.queensu.ca

The preparation of chiral solid materials is an important step in understanding how molecular chirality is transmitted in condensed phases.[1] Research into structures that are not inherently flat[1] is limited to a few examples[2] and has focused heavily on the preparation of purely inorganic structures.[3] With a few notable exceptions,[4] these materials are generally prepared in either a racemic or slightly enantiomerically enriched state, and chirality is introduced *exogenously* through the use of chiral templates or surfactants. Recent efforts in the area of organosilicate materials[5] provide an opportunity to introduce chirality directly into the backbone of the material by polymerization of chiral monomers.[6,7]

Polyorganosiloxanes are a well-known class of organic−inorganic composite materials in which siloxane units are bridged by organic backbones.[8] When the polymerization of such organosiloxanes is carried out in the presence of a surfactant template, order and porosity are introduced and remain after removal of the surfactant.[9] The resulting periodic mesoporous organosilicates (PMOs)[5] differ from conventional materials such as MCM-41[9b] or SBA-15[9c] in that organic molecules are integrated into the walls of the material.[10]

In addition to surfactant-templated approaches to ordered PMOs, Moreau and Man have prepared self-templated organic/inorganic composite materials which have highly ordered helical morphologies on the macroscopic level.[11] Surfactant-templated PMOs employing chiral molecules as the building blocks, however, are rare. Chiral materials have been prepared by incorporation of chiral salen complexes,[6a] binaphthyl species,[6b] hydroborated alkenes,[6c] and tartaric acid derived species[6d] decorated with siloxanes; however, silica (in the form of TEOS, $Si(OEt)_4$) is virtually always employed, making up more than 70% of the material in most cases. In rare cases that do not require TEOS as the bulk constituent, racemization is observed under the harsh synthetic conditions routinely employed for condensation.[7]

We report herein a fundamentally different approach for the introduction of chirality into ordered materials, in which a chiral dopant is employed to induce chirality in the bulk material. This work also represents the first preparation and characterization of a PMO material derived from axially chiral biphenyl units.

For the bulk material, 4,4′-bis-(triethoxysilyl)biphenyl (**1**) was employed, which has been used in the preparation of achiral PMO materials.[12] This monomer is interesting since it can adopt chiral conformations by rotation around the central C−C single bond.[13] For example, in the two most stable polymorphs of crystalline 4,4′-*tert*-butylbiphenyl (**2**), the dihedral angle about the central C−C bond is ca. 40°, similar to the minimum energy chiral conformation of biphenyl observed in the gas phase.[14] With a rotational barrier about this bond of ∼10−15 kcal/mol in the solid state, we envisaged biasing one conformer of these species in the solid state via co-condensation with a homochiral additive.

Thus a chiral mesoporous material composed primarily of **1** was prepared, along with varying levels of a chiral, resolvable biaryl

Chart 1. Biaryl Structures in Materials and Chirality Transfer

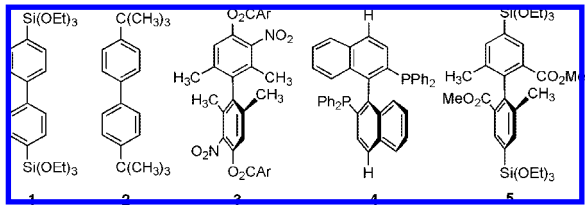

dopant. A 2,2′,6,6′-substituted biphenyl was chosen because the high rotational barrier about the central C−C bond (ca. 40 kcal/mol) should prevent racemization. Furthermore, the biaryl motif has been shown to be highly effective at transmitting chirality. For example, compound **3** (Chart 1) is a very effective chiral dopant in smectic liquid crystal hosts with biaryl core structures,[15a] and ligands such as Binap[15b] (**4**) are highly effective at transmitting chirality through asymmetric catalysis. Hence, enantiomerically pure axially chiral species **5** became our target structure.

Compound **5** was prepared from commercially available 2-nitro-3-methylbenzoic acid (**6**) using an Ullman coupling reaction as the key step in the formation of the biaryl bond.[16] After resolution, the *M* and *P* enantiomers of **7** were treated with $NaNO_2$ and HI in DMSO, yielding the corresponding diiodides **8** (Scheme 1). The $Si(OEt)_3$ units were introduced via a Rh-catalyzed reaction. Under optimized conditions, both enantiomers of **5** were prepared in up to 80% yield.

Scheme 1. Synthesis of Enantiomerically Pure Monomer **5**

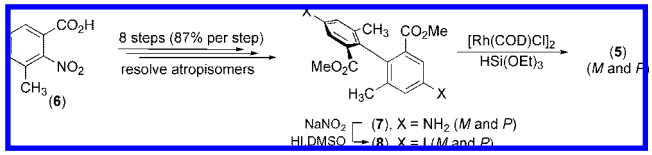

Using Brij-76 as the surfactant, co-condensation of racemic **5** and achiral **1** in a 15:85 ratio produced ordered porous materials with pore sizes of ca. 25 Å *without the addition of an inorganic silica source* (Table S-1 and Figure S-1). The powder X-ray diffraction pattern reveals an intense peak below 2θ with a *d*-spacing of 52.5 Å indicating that the material exhibits mesoporosity (Figure S-2). The TEM image shown in Figure 1a reveals a 2D ordered porous material with an estimated lattice constant of 60 Å, consistent with that calculated from pXRD data (52.5 Å).

^{29}Si CP MAS NMR (Figure 1b) displays only T-type resonances, indicating that cleavage of the Si−C bonds did not occur during the synthesis of the material. ^{13}C CP MAS NMR and IR spectra both confirmed the presence of the substituted biphenyl derived from **5** (Figures S-3 and S-4).

Having identified the requisite bulk characteristics of the racemic PMO material, the synthesis was repeated using both enantiomers

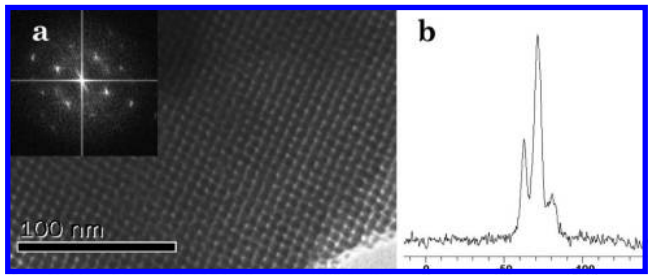

Figure 1. Racemic material **QChiMat-15**. (a) TEM image and (b) ^{29}Si CP-MAS NMR indicating no Si−C bond cleavage.

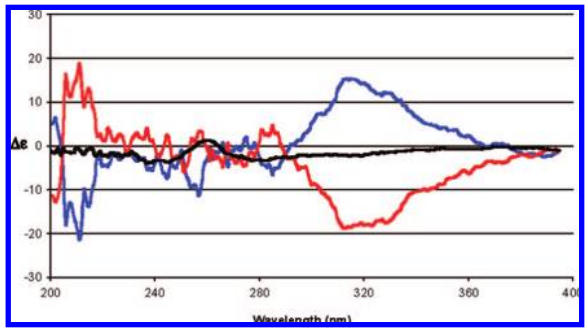

Figure 2. CD spectra of chiral materials derived from (+) and (−) **5**, in either **1** as the main component (blue/red) or SiO_2 (black).

of **5** (eq 1). The chirality of the resulting materials (**QChiMat-15**) was assessed by examination of their CD spectra as amorphous powders dispersed in KBr pellets.[17] As expected, mirror image CD spectra were obtained when opposite enantiomers of **5** were employed (Figure 2).

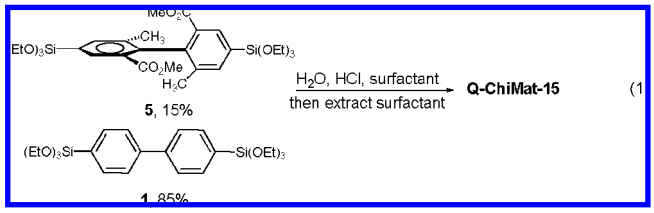

The strongest CD signal observed in **QChiMat-15** appears at ca. 315 nm, significantly red-shifted compared to the UV spectra of both monomers (**1**, $\lambda_{max} = 260$ nm, **5**, $\lambda_{max} = 258$ nm). A related absorption is also observed in the solid state UV spectrum of the materials (**QChiMat-30** and **100** are shown in Figure S-5) confirming that this signal is not an artifact. To determine the origins of this signal, a material was prepared using *silica* as the main constituent and **5** as the sole organic component: co-condensation of **5** (15%) with $Si(OEt)_4$ (85%) carried out under identical conditions results in **QChiMat-SiO$_2$** (eq 2). In this material, no CD signal is observed at 315 nm, but one weak absorption appears at 260 nm (Figure 2, black).

5, 15% + $Si(OEt)_4$, 85% $\xrightarrow[\text{then extract surfactant}]{H_2O,\ HCl,\ \text{surfactant}}$ **Q-ChiMat-SiO$_2$** (2)

Interestingly, hydrothermal treatment of **QChiMat-15** results in a complete loss of the signal at 315 nm (Figure 3, blue/red) and is characterized by a weak peak at 260 nm, overlapping with the signal from **QChiMat-SiO$_2$** (pale blue). Considering these data, the signal at 315 nm is reasonably assigned to an aggregate species consisting of **5** and one or more units of **1** in the solid state.[18] The loss of this signal upon hydrothermal treatment is consistent with a restructuring

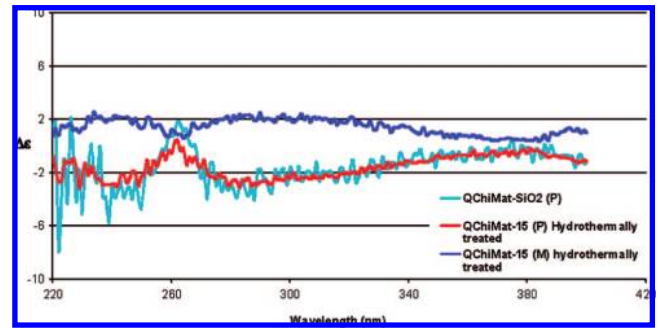

Figure 3. CD spectra of **QChiMat-SiO$_2$** and of **QChiMat-15** ((+) and (−)) after hydrothermal treatment.

of the material that disrupts the interaction between **1** and **5** in the solid state.[19] Consistent with the predicted rotational barriers, the axially chiral biphenyl units derived from **5** are configurationally stable under these conditions: treatment of the resolved bis-siloxane precursor **5** under identical conditions (boiling water, 24 h) did not cause any loss of optical activity (Figure S-6).

QChiMat-30 and **QChiMat-100** were also prepared, in which 30% and 100% of the axially chiral biphenyl monomer **5** was employed. In the case of **QChiMat-30**, the most prominent signal was again the signal at 315 nm, along with signals corresponding to the isolated biaryl at 260 and 240 nm (Figure S-7). In the case of **QChiMat-100**, the peak at 315 nm was again absent (Figure S-8), supporting the hypothesis that this is attributed to an interaction between **1** and **5**. This signal is also absent in the UV spectrum of **QChiMat-100** (Figure S-5) although present in the 30% material, further supporting its assignment as resulting from a chiral structure resulting from the interaction of **1** and **5** (Scheme 2).[20]

Scheme 2. Dimeric Structures Employed in DFT Calculations as Models of Chiral Interactions in the Solid State and Relationship Between the Distance Between the Carbon Atoms of the Central Bond in **11** (d_{C-C}) and Calculated λ_{max}[21]

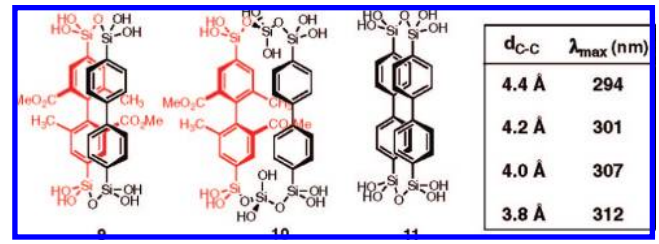

Dimeric structures **9**−**11** were examined as models of the full material, and their CD spectra simulated using time-dependent density functional theory calculations at the B3LYP/6-31++G(d,p) level of theory (Scheme 2). Although TEOS was not employed in any materials synthesis, compound **10**, with an extra silicon unit in between the biaryls, was examined as a model of the alternating biaryl structures proposed by Inagaki and co-workers.[12a] The simulated CD spectra (Figure S-9) are in good agreement with experimental CD and UV spectra.

The calculated spectrum of **5** exhibits a peak at 251 nm, which is similar to the observed solution phase signal at 258 nm. The CD spectra of dimeric species **9** and **11** are both red-shifted to 281 and 288 nm, respectively, indicating electronic delocalization between the adjacent biaryl rings in both cases. The 288 nm signal calculated for **11** is reasonably close to the observed value of 280 nm for the UV spectrum of a PMO prepared entirely from **1** (Figure S-10), especially considering the uncertainty in both the experimental and calculated data.[21]

The excitations associated with the longest wavelength peaks in the spectra of **9** and **11** involve electronic transitions within the π systems of each biphenyl component, as well as between adjacent phenyl rings. This is shown in the MO diagrams for the electronic transitions contributing to the peak at 287.8 nm in the CD spectrum of **11** (Figure S-11). The excitations associated with the low energy peaks in the CD spectra of **10** involve electronic transitions occurring primarily within the π systems of each biphenyl component, with minimal electron transfer between adjacent phenyl rings.

A series of calculations were performed on **11** varying the distance (d_{C-C}) between the carbon atoms of the biaryl bond (Scheme 2). As the two biaryls are moved closer together and d_{C-C} is decreased from 4.4 to 3.8 Å, the wavelength of the lowest energy peak shifts systematically from 294 to 312 nm, which is remarkably close to the 315 nm signal observed in **QChiMat-15**.

These results indicate that the formation of complexes in which the adjacent phenyl rings are well-aligned and sufficiently close for electronic transitions to occur between the rings increases the absorption wavelengths observed in the CD spectra. Thus, there are likely regions within **QChiMat-15**-type materials where the two monomers are forced to interact closely with one another. Interestingly, the calculated formation energy of dimer **9** is higher than that of **10**, which may explain the loss of the signal at 315 nm when the material is hydrothermally treated, and reorganizes into a lower energy state in which the aryl rings are further apart.

In conclusion, we have demonstrated that chiral mesoporous materials can be prepared using a combination of 4,4′-bis(triethoxysilyl)biphenyl and axially chiral, enantiomerically pure biphenyl derivatives of similar structure. The resulting materials retain the chirality of the dopant and, in addition, contain regions in which the dopant appears to influence the structure of the biphenyls resulting in new chiral aggregates within the material. To the best of our knowledge, this is the first example of a chiral PMO prepared with an axially chiral monomer and the first example of chirality transfer within a PMO material. The application of these materials in catalysis and separation science is ongoing in our laboratories.

Acknowledgment. The authors acknowledge Abdelhamid Sayari for helpful discussions. The work was supported by the Natural Sciences and Engineering Research Council of Canada (NSERC), Silicycle Inc., and the Merck Frosst Center for Therapeutic Research. Computing resources were made available by the Shared Hierarchical Academic Research Computing Network (SHARCNET: www.sharcnet.ca).

Supporting Information Available: Synthetic procedures; computational methods; full details on the characterization of the materials; CD spectra for 30% and 100% material; simulated CD spectra for **1**, **5**, and **9**−**11**; and TEM images. This material is available free of charge via the Internet at http://pubs.acs.org.

References

(1) (a) Lavoie, S.; Laliberté, M.-A.; Temprano, I.; McBreen, P. H. *J. Am. Chem. Soc.* **2006**, *128*, 7588–7593. (b) Ahmadi, A.; Attard, G.; Feliu, J.; Rodes, A. *Langmuir* **1999**, *15*, 2420–2424.
(2) Marx, S.; Avnir, D. *Acc. Chem. Res.* **2007**, *40*, 768–776.
(3) Che, S.; Liu, Z.; Ohsuna, T.; Sakamoto, K.; Terasaki, O.; Tatsumi, T. *Nature* **2004**, *429*, 281–284.
(4) (a) Yokoi, T.; Yamataka, Y.; Ara, Y.; Sato, S.; Kubota, Y.; Tatsumi, T. *Microporous Mesoporous Mater.* **2007**, *103*, 20–28. (b) Qiu, H. B.; Wang, S. G.; Zhang, W. B.; Sakamoto, K.; Terasaki, O.; Inoue, Y.; Che, S. *J. Phys. Chem. C* **2008**, *112*, 1871–1877. (c) Jung, J. H.; Ono, Y.; Hanabusa, K.; Shinkai, S. *J. Am. Chem. Soc.* **2000**, *122*, 5008–5009. (d) Yang, Y. G.; Suzuki, M.; Owa, S.; Shirai, H.; Hanabusa, K. *J. Am. Chem. Soc.* **2007**, *127*, 581–587.
(5) (a) Inagaki, S.; Guan, S.; Fukushima, Y.; Ohsuna, T.; Terasaki, O. *J. Am. Chem. Soc.* **1999**, *121*, 9611–9614. (b) Asefa, T.; MacLachlan, M. J.; Coombs, N.; Ozin, G. A. *Nature* **1999**, *402*, 867. (c) Melde, B. J.; Holland, B. T.; Blanford, C. F.; Stein, A. *Chem. Mater.* **1999**, *11*, 3302.
(6) (a) Baleizao, C.; Gigante, B.; Das, D.; Alvaro, M.; Garcia, H.; Corma, A. *Chem. Commun.* **2003**, 1860–1861. (b) Alvaro, M.; Benitez, M.; Das, D.; Ferrer, B.; Garcia, H. *Chem. Mater.* **2004**, *16*, 2222–2228. (c) Ide, A.; Voss, R.; Scholz, G.; Ozin, G.; Antonietti, M.; Thomas, A. *Chem. Mater.* **2007**, *19*, 2649–2657. (d) Garcia, R. A.; van Grieken, R.; Iglesias, J.; Morales, V.; Gordillo, D. *Chem. Mater.* **2008**, *20*, 2964–2971.
(7) Inagaki, S.; Guan, S. Y.; Yang, Q.; Kapoor, M. P.; Shimada, T. *Chem. Commun.* **2008**, 202–204.
(8) Loy, D. A.; Shea, K. J. *Chem. Rev.* **1995**, *95*, 1431–1442.
(9) Yanigasawa, T.; Shimizu, T.; Kuroda, K.; Kato, C. *Bull. Chem. Soc. Jpn.* **1990**, *63*, 988–992. (b) Beck, J. S.; Vartuli, J. C.; Roth, W. J.; Leonowicz, M. E.; Kresge, C. T.; Schmitt, K. D.; Chu, C. T. W.; Olson, D. H.; Sheppard, E. W.; Mccullen, S. B.; Higgins, J. B.; Schlenker, J. L. *J. Am. Chem. Soc.* **1992**, *114*, 10834–10843. (c) Yang, P. D.; Deng, T.; Zhao, D. Y.; Feng, P. Y.; Pine, D.; Chmelka, B. F.; Whitesides, G. M.; Stucky, G. D. *Science* **1998**, *282*, 2244–2246.
(10) Fujita, S.; Inagaki, S. *Chem. Mater.* **2008**, *20*, 891–908.
(11) Moreau, J. J. E.; Vellutini, L.; Man, M. W. C.; Bied, C. *J. Am. Chem. Soc.* **2001**, *123*, 1509–1510.
(12) (a) Kapoor, M. P.; Yang, Q.; Inagaki, S. *J. Am. Chem. Soc.* **2002**, *124*, 15176–15177. (b) Sayari, A.; Yang, Y. *Chem. Mater.* **2007**, *19*, 4117–4119.
(13) Almenningen, A.; Bastiansen, O.; Fernholt, L.; Cyvin, B. N.; Cyvin, S. J.; Samdal, S. *J. Mol. Struct.* **1985**, *128*, 59.
(14) Näther, C.; Jess, I.; Havias, Z.; Bolte, M.; Nagel, N.; Nick, S. *Solid State Sci.* **2002**, *4*, 859.
(15) (a) Lemieux, R. P. *Acc. Chem. Res.* **2001**, *34*, 845–853. (b) Noyori, R. *Angew. Chem., Int. Ed.* **2002**, *41*, 2008–2022.
(16) Montoya-Pelaez, P. J.; Uh, Y.-S.; Lata, C. J.; Thompson, M. P.; Lemieux, R. P.; Crudden, C. M. *J. Org. Chem.* **2006**, *71*, 5921.
(17) CD spectra of solid samples can give rise to artifacts due to ordering of microcrystalline domains. However our materials are amorphous, not crystalline. Furthermore, the signal at 315 nm is close to a UV absorption in the same material (Supporting Information) which is further proof this is not an artifact. Kuroda, R.; Honma, T. *Chirality* **2000**, *12*, 269–277.
(18) (a) Nam, H.; Boury, B.; Park, S. Y. *Chem. Mater.* **2006**, *18*, 5716–5721. (b) Ben, F.; Boury, B.; Corriu, R. J. P. *Adv. Mater.* **2002**, *14*, 1081–1084.
(19) This likely occurs by cleavage/reformation of the silicon−oxygen bonds and subsequent reorganization of the material: Burleigh, M. C.; Markowitz, M. A.; Jayasundera, S.; Spector, M. S.; Thomas, C. W.; Gaber, B. P. *J. Phys. Chem. B* **2003**, *107*, 12628–12634.
(20) Materials with less than 15% of **5** did not show signals in the CD spectra.
(21) The calculations yield CD spectra for structure **11** because static DFT was employed, and the structure optimized for a single enantiomer at 0 K. At this temperature, there is insufficient energy for the bond rotation to interconvert between the two enantiomeric conformations.

JA804866E